J Mater Sci: Mater Med (2010) 21:393–398
DOI 10.1007/s10856-009-3874-2

Rapid biomineralization of chitosan microparticles to apply in bone regeneration

A. Champa Jayasuriya · Shane Kibbe

Received: 9 July 2009 / Accepted: 9 September 2009 / Published online: 16 September 2009

Abstract The aim of this study was to prepare bone like mineral (BLM) layers rapidly on the exterior surfaces of chitosan (CS) microparticles (MPs). The CS MPs were fabricated using a scale-up double emulsification method. The CS MPs were in the spherical shape and the size of 30–60 μm. The MPs were then placed in 5× concentrated simulated body fluid (5 × SBF) and allowed to undergo biomineralization to form a BLM layers on the surface of CS MPs at 37°C over a 24 h period. The BML layers on the exterior surface of CS MPs were characterized using wide angle X-ray diffraction (XRD), Fourier transform infrared microscopy (FTIR), and scanning electron microscopy (SEM). Insulin like growth factor-1 (IGF-1) was dissolved at a concentration of 1 μg/ml in 5 × SBF to incorporate into the BLM layer. The CS MPs (100 mg) were incubated in a sample of 4 ml of 5 × SBF containing IGF-1 at a concentration of 1 μg/ml for 24 h. The IGF-1 release from BML layers on CS MPs were studied by placing MPs in 4 ml of phosphate buffered saline (PBS) and incubating MPs at 37°C for 30 days. Samples (100 μl) were taken over the course of the 30 days and analyzed using Enzyme-linked Immunosorbent assay (ELISA). The release IGF-1 from BML layers was in a burst manner followed by a sustained release during the 30-day period. This study suggests that the CS MPs have the potential to be used to help deliver therapeutic drugs to localized areas and hence increase and accelerate bone growth.

A. C. Jayasuriya (✉) · S. Kibbe
Department of Orthopaedics, University of Toledo,
3065 Arlington Avenue, Dowling Hall # 2447, Toledo,
OH 43614-5807, USA
e-mail: a.jayasuriya@utoledo.edu

1 Introduction

Bone like mineral (BLM) is a carbonate containing hydroxyl apatite that closely resembles hydroxyapatite, a major component in mammalian bones [1]. A BLM layer can be formed on the surface of bioactive materials by soaking in simulated body fluid (SBF), which is a solution containing inorganic ion concentrations nearly equal to those of human blood plasma. One of the advantages of using a biomimetic method to form BLM is that the biologically active molecules can be co-precipitated with inorganic components. This process may form an organic–inorganic matrix due to gentle conditions throughout the process. Therefore, these matrices can be used as carriers for a variety of molecules, such as proteins including drugs and growth factors [2–5].

In the conventional biomimetic process, BLM layers can be deposited onto the biodegradable polymer surfaces by soaking them in SBF for 16 days or more. Recently we have accelerated the biomimetic process to deposit BLM layers in 3D porous poly(lactic-co-glycolic acid) (PLGA) scaffold surfaces [6]. The BLM was deposited on PLGA scaffolds within 36–48 h by modifying the biomimetic process parameters and applying surface treatments into PLGA scaffolds.

Microparticles (MPs) have been studied as delivery vehicles for drugs, proteins and genes using different materials, such as chitosan (CS) [7–9]. Recently, MPs were investigated as injectable scaffolds for cartilage and bone regeneration [10–12]. The MPs can be seeded with autologous cells before implantation to function as cell carriers. MPs were also designed to enhance host cell migration, attachment, proliferation, and differentiation once implanted.

CS is a deacetylated derivative of chitin, a high molecular weight and the second most abundant natural

biopolymer commonly found in shells of marine crustaceans and cell walls of fungi [13]. In general, these materials evoke a minimal foreign body reaction [13], with little or no fibrous encapsulation. Biodegradability and biocompatibility are very important properties that make CS useful material for bone regeneration. In this study, we selected CS based on its favorable properties to fabricate the MPs using our scale-up procedure [14]. We also selected insulin-like growth factor-1 (IGF-1), which stimulates osteoblast proliferation and new bone growth at local site [15], to incorporate into BLM layers on MPs. IGF-1 is a differentiation factor for osteoblasts as well as a proliferative stimulus for chondrocytes and pre-osteoblasts. In rat calvarial explant cultures, IGF-1 increased collagen synthesis, matrix apposition, and cell replication [16]. We have also observed that IGF-1 incorporated BLM on PLGA scaffolds were enhanced the mesenchymal stem cell (MSC) attachment and proliferation compared to unmineralized PLGA scaffolds [17].

With our previous experience on rapid biomineralization of PLGA scaffolds, we developed biomimetic strategies to nucleate and grow a continuous BLM in the exterior surface of CS MPs using 5 × SBF via a one-step room temperature process. In this paper, we report rapid biomineralization on the exterior surfaces of CS MPs, characterization of mineralized MPs, and release of IGF-1 from BLM layers on exterior surfaces of MPs.

2 Materials and methods

2.1 Materials

The CS (85% deacetylated), Sodium tripolyphosphate (TPP), Cottonseed oil, hexane, acetic acid, and Span 85 used to fabricate the MPs were purchased from Sigma chemical company (Milwaukee). Acetone was purchased from Fisher Scientific Company. IGF-1 and phosphate buffered saline (PBS) were purchased from Biovision and Invitrogen companies, respectively.

2.2 Fabrication of MPs

The hybrid MPs were fabricated using our scale-up procedures as described previously [14]. Briefly, the CS solution (1.5%, w/v) was prepared by dissolving CS in dilute acetic acid (1%, v/v) at room temperature and filtering through nylon cloth to remove any insoluble components. The CS solution (25 ml) was diluted 1:1 by volume with acetone, and then 36 ml of this mixture was added drop wise into a mixture containing 600 ml of Cottonseed oil and 4 ml of span 85. The oil suspension was stirred for 14 h at 37°C and an agitation speed of 870 rpm. 64% (w/w) of TPP was mixed with 4 ml dH_2O and added to the reaction mixture. Four hours after the addition of TPP, the MPs were purified using hexane followed by vacuum filtration and air drying. It should be noted that some CS MPs for FTIR and XRD analysis were fabricated without TPP using a normal fabrication procedure (without scale-up) [14]. We use TPP as a cross-linking agent to fabricate the chitosan microparticles. When we use TPP, we are able to scale-up the yield of microparticles without a problem. However, if we do not use TPP we cannot successfully scale up the microparticles. The mineralized microparticles were prepared using TPP. However, in order to observe the peaks related to biomimetic mineral in XRD and FTIR we did not use TPP, because of TPP showing the similar peaks to biomimetic mineral in XRD and FTIR.

2.3 Preparation of simulated body fluid (SBF)

SBF was produced to give ion concentrations that are similar to blood plasma (Table 1). We prepared a 5 × SBF, which means we increased the concentrations of chemicals by a factor of five. The chemicals from the Table 1 were mixed into deionized water using a stirring plate at room temperature. The pH was buffered to 6.8 using 1 M sodium hydroxide (NaOH).

2.4 Surface modification

Before we attempted to integrate IGF-1 into the BLM layers on the surface of MPs, we first treated the MPs to allow surface modifications which would facilitate better deposition of BLM. The MPs were soaked in 0.1 M NaOH solution for 20 min. The NaOH served to increase functional groups such as hydroxyl groups on the surface of CS. The MPs were rinsed thoroughly with deionized water to ensure that no NaOH was left behind.

Table 1 Ion concentrations (in mM) of blood plasma and simulated body fluids (SBF)

	Na^+	K^+	Mg^{2+}	Ca^{2+}	Cl^-	HCO_3^-	$H_2PO_4^-$	SO_4^{2-}	pH
Blood plasma	142.0	5.0	1.5	2.5	103.0	27.0	1.0	0.5	7.2–7.4
1 × SBF	141.0	5.0	1.5	2.5	152.0	4.2	1.0	0.5	7.4
5 × SBF	705.0	25.0	7.5	12.5	760	21.0	5.0	2.5	6.8

2.5 BLM morphology—scanning electron microscope (SEM)

Morphology of BLM layers on the surface of MPs was obtained using a Hitachi S3200 SEM operating with a 15–20 kV accelerating voltage under high vacuum. A conventional secondary electron scintillator detector was used with a tungsten filament. The MPs were coated with a 20 nm gold layer using a Denton vacuum model Desk II sputter coater. The morphology of CS MPs including the size, shape, and surface properties was examined using a SEM.

2.6 Chemical structure of BLM–fourier transform infra red (FTIR)

The CS MPs which were prepared without TPP were ground into a fine powder and blended with KBr and then pressed to make a pellet which was used for FTIR measurements. The measurements were performed with 4 cm^{-1} resolution with FTIR Perkin Elmer spectroscopy.

2.7 Physical structure of BLM—wide angle X-ray diffraction (XRD)

A Rigaku X-ray diffractometer was used with a Cu-K_α target to determine the physical structure of the MPs. The X-ray generator was operated at 40 kV voltage and 100 mA current. XRD patterns were obtained between 2θ angle range 10–60° with a scan speed of 2°/min and a step size of 0.02°.

2.8 Incorporation of IGF-1 into BLM on MPs

IGF-1 was incorporated into 5 × SBF at a concentration of 1 μg/ml. MPs (100 mg) were placed in the 4 ml of 5 × SBF containing IGF-1 for 24 h at 37°C.

2.9 In vitro release kinetics of IGF-1

The mineralized MPs (100 mg) were incubated in PBS medium (4 ml) at 37°C and maintained a low stirring motion (50 rpm) within the incubator. Samples were taken in triplicate at predetermined times up to 30 days. We used 100 μl per sample and after the samples were taken we replaced PBS into the test tube to keep the same volume throughout the incubation period. Samples were recorded and then stored in the freezer until perform the ELISA assay.

After all the samples were taken we used an R & D Systems Human IGF-1 Enzyme-linked Immunosorbent Assay (ELISA) kit to determine the amount of IGF-1 released within each sample. We followed the manufacture's protocol directions to performed ELISA. An ELISA plate reader was used to determine the optical density of the samples at 540 nm. A standard curve was established using different concentrations of IGF-1 solution to determine the amount of IGF-1 released from the BLM layers.

3 Results

3.1 Mineralized MP morphology—SEM

SEM images revealed that CS MPs were approximately spherical in shape with a diameter range of 30–60 μm seen in Fig. 1a. In addition, MPs have shown the smooth outer surface without any porous structure. To study BLM formation on the exterior surfaces of CS MPs, MPs were soaked at 37°C in 5 × SBF for 24 h. A SEM image has demonstrated the growth of a continuous mineral layer on

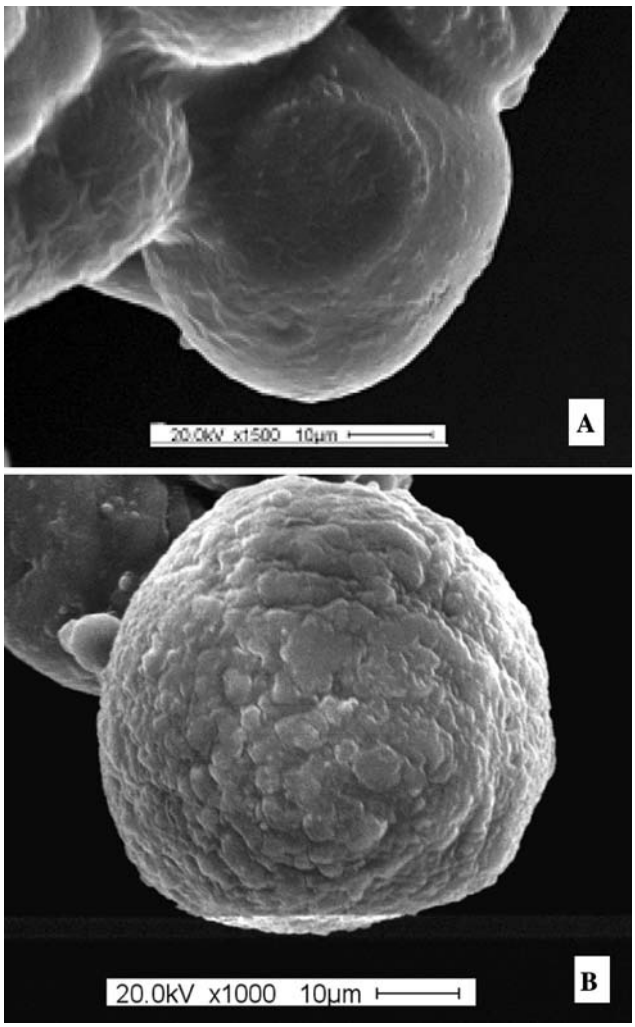

Fig. 1 SEM images of CS MPs before mineralization (**a**) and after mineralization (**b**)

the surface of MPs after 24 h mineralization in Fig. 1b. It seems that the mineral deposition layer was not affected for MPs shape.

3.2 Evidence of having BLM layers on CS MPs—FTIR

Chemical composition of CS MPs was determined using FTIR (Fig. 2). IR spectra exhibit the purified CS (bulk), CS MPs, and mineralized (24 h in 5 × SBF) CS MPs. None of the MPs were cross-linked with TPP. FTIR spectrum for CS bulk sample shows a broad peak for at 1627 cm^{-1} indicating the combination of Amide I peak and a shoulder peak for amide II band (Fig. 2). Another broad peak appeared at 3413 cm^{-1} due to the amine N–H symmetrical vibration. The peaks at 887 and 1130 cm^{-1} are corresponded to the saccharide structure of the CS. FTIR spectrum of MPs exhibited high intensity peaks or new peaks compared to bulk CS sample. Characteristic amide I and amide II peaks appeared at 1648 and 1566 cm^{-1} [18], respectively for MPs containing 0% TPP and mineralized CS MPs. In addition, the characteristic phosphate band at 605 cm^{-1} appeared for mineralized CS MPs, confirming the presence of phosphate groups. It seems that the characteristic peaks for CO_3^{2-} at 1630 (v_3), 1551 (v_3) and PO_4^{3-} at 1037 (v_3) [19] are overlapped with the characteristic peaks related to CS.

3.3 Physical structure of BLM layers on CS MPs—XRD

BLM formation on the exterior surfaces of CS MPs was examined using wide-angle XRD. The CS stock sample

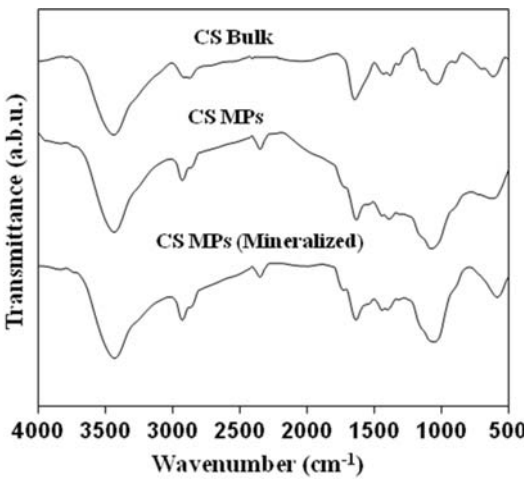

Fig. 2 FTIR spectra of the CS-bulk; CS MPs (without cross-linking with TPP); and mineralized CS MPs (without cross-linking with TPP)

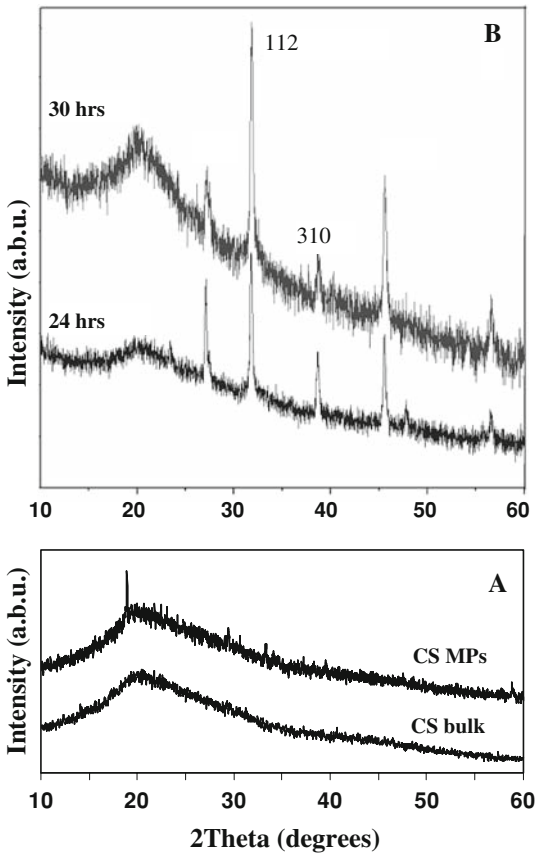

Fig. 3 XRD patterns for CS-bulk; CS MPs (**a**); mineralized MPs at 30 and 24 h (**b**)

exhibited the main peak at $2\theta = 20°$ in XRD pattern in Fig. 3a. This peak was clearly exhibited in the same region of XRD due to the existence of CS in the CS MPs (Fig. 3a). In addition, XRD patterns of CS MPs were shown a few other peaks in $2\theta = 10$–$40°$ region, confirming the presence of TPP in the CS MPs (Fig. 3a).

Since TPP contains the phosphate groups, XRD peaks of phosphate groups from TPP were similar to that of BLM. The XRD peaks of BLM were difficult to identify since they were not well resolved from the phosphate peaks. Therefore, we prepared the MPs without ionic cross-linking with TPP to determine the XRD peaks for BLM coated on the exterior surfaces of MPs (Fig. 3b). The CS MPs mineralized for 24 h exhibited the high intensity XRD peaks evidencing the mineral deposition compared to the CS MPs soaked in SBF for 30 h. Generally, more mineral deposition on the material surface can be expected when the incubation time in SBF increases. XRD patterns of BLM-coated CS MPs exhibited the peaks at $2\theta = 32.2°$, 39.2° corresponding to the (112) and (310) hydroxyapatite planes in the bone matrix [6]. In addition, several intense XRD peaks appeared at $2\theta = 23.3°$, 27.2°, and 46°. The peaks at $2\theta = 23.3°$, and 46° corresponded to the XRD

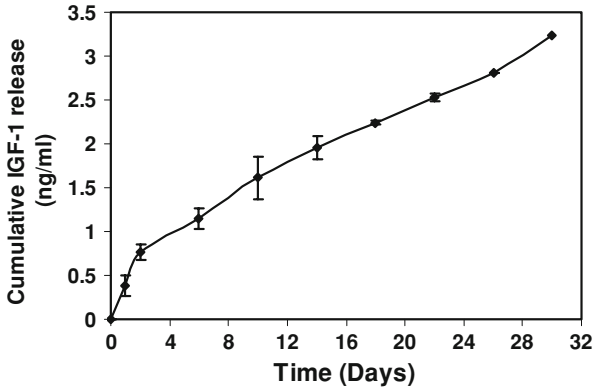

Fig. 4 Cumulative release of IGF-1 from BLM on the exterior surface of CS MPs

peaks of synthetic carbonated apatite. These results suggest that the diffraction patterns of mineralized MPs display evident similarities and point out the analogy between the structures of bone bioapatite [6] and synthetic carbonated apatite [20].

3.4 IGF-1 release-ELISA assay

The cumulative IGF-1 release was examined as a function of incubation time and plotted in a Fig. 4. The cumulative release amount of IGF-1 was increased up to 30 days. Approximately 0.8 ng/4 μg of IGF-1 was released during the first 2 days of incubation and approximately 3.2 ng/4 μg was released by day 30 of the incubation period. IGF-1 release from the mineral layer seems to be a burst release within the first 2 days followed by a sustained release up to 30 day period. Within 2 days, ~25% IGF-1 was released compared to the total amount released at 30 days.

4 Discussion

In this study, we were able to accelerate the deposition of biomimetic BLM on the surfaces of CS MPs within 24 h incubation in 5 × SBF. We increased the ionic concentrations respectively by a factor of five to produce a 5 × stock solution of SBF. By increasing the concentrations of the ions we created a way to accelerate the mineralization of the MPs to create a BLM similar to our previous study [6]. In our previous study we were able to deposit BLM on the surfaces of porous PLGA scaffolds within 36–48 h. Another integral part of accelerating the formation of BLM layers on the surface of CS MPs was to undergo surface modification using NaOH. The NaOH allowed for carboxyl acid and hydroxyl groups to form which help facilitate deposition of ions.

The acceleration of biomineralization provides short time exposure of the therapeutic drugs and growth factors with 5 × SBF compared to traditional long incubation periods. Therefore, bioactivity of those reagents can also be protected in addition to possible contamination with long period incubation of biological reagents. Another advantage is that the waste of therapeutic drugs and growth factors can be avoided using short time mineralization. Hence it provides economically benefit since most therapeutic reagents are very expensive. In addition, systemic delivery waste and side effects can be avoided when therapeutic agents are delivered at the local site.

We also observed that the higher amount of IGF-1 released from CS MPs relative to the total amount of IGF-1 amount used for drug loading, compared to PLGA scaffolds during 30-day period. Cumulative IGF-1 release amount of BLM in CS MPs and PLGA scaffolds was 3.3 ng/4 μg and 1.1 ng/7.5 μg, respectively during 30 days. This result can be explained as follows. When we compared the biomineralization of CS MPs versus porous PLGA scaffolds, uniform BLM layers can be deposited on the exterior surfaces of CS MPs. On the other hand, the BML deposition may not uniform between the exterior surfaces of PLGA scaffolds and interior pore surfaces. The uniform BLM layers on the exterior surface of CS MPs may contribute for the uniform drug and growth factor loading across the mineral layer and hence more predictable release. In addition, uniform coating of BLM layers were not affected for the shape of the CS MPs as seen our results (Fig. 1b).

Creating a bio-compatible surface for the newly forming bone reduces patient recovery time by facilitating rapid bone formation around the implant. Studies have shown that, this new coating binds more tightly to bone than mineral-coated implants produced by conventional methods [4, 21]. This type of apatite layer is not observed at the interface between non-bioactive materials and bone. Non-bioactive materials typically do not exhibit surface-dependent cell differentiation [22]. Co-precipitation allows the incorporation of IGF-1 into mineral layers on CS MPs. Our results have shown that IGF-1 can be released from the BLM layers on the surface of the CS MPs. The nanogram level of IGF-1 and has shown mitogenic and osteogenic effects in cell culture experiments [23, 24].

The main advantage of MP approach, compared with the traditional block scaffolds, is that small particles can be combined with a vehicle and be administered by injection, thus giving the possibility of filling defects of different shapes and sizes through minimally invasive surgery [25, 26]. Minimally invasive surgeries limit the pain, prolonged hospitalization, recovery time, blood loss, and scar formation compared with conventional open surgeries, which require implanting 3D conventional scaffolds.

5 Conclusions

In this study, we have shown that we were able to accelerate the formation of BLM layers on the exterior surface of CS MPs at normal pressure and temperature. IGF-1 was shown to be released from the BLM on the exterior surface of the CS MPs in a burst release manner first, and then maintained sustained release. The acceleration of BLM on CS MPs provides the protection of loaded drugs or growth factors against bioactivity and contamination, and economical benefit, from long-term incubation. The drug or growth factor loaded BLM layers on CS MPs can be potentially applied to the local defect site using a suitable injection.

Acknowledgements We would like to acknowledge the National Science Foundation (NSF) for providing partial financial support to accomplish this work with NSF Grant Number 0652024.

References

1. De Bruijn JD, van Blitterswijk CA, Davies JE. Initial bone matrix formation at the hydroxyapatite interface in vivo. J Biomed Mater Res. 1995;29:89–100.
2. Wen HB, Moradian-Oldak J. Modification of calcium-phosphate coatings on titanium by recombinant amelogenin. J Biomed Mater Res. 2003;64:483–90.
3. Liu Y, Hunziker EB, Randall NX, de Groot K, Layrolle P. Proteins incorporated into biomimetically prepared calcium phosphate coatings modulate their mechanical strength and dissolution rate. Biomaterials. 2003;24:65–70.
4. Wen HB, de Wijn JR, van Blitterswijk CA, de Groot K. Incorporation of bovine serum albumin in calcium phosphate coating on titanium. J Biomed Mater Res. 1999;46:245–52.
5. Stigter M, Bezemer J, de Groot K, Layrolle P. Incorporation of different antibiotics into carbonated hydroxyapatite coatings on titanium implants, release and antibiotic efficacy. J Control Release. 2004;99:127–37.
6. Jayasuriya AC, Shah C, Ebraheim NA, Jayatissa AH. Acceleration of biomimetic mineralization to apply in bone regeneration. Biomed Mater. 2008;3:015003.
7. Varde NK, Pack DW. Microspheres for controlled release drug delivery. Expert Opin Biol Ther. 2004;4(1):35–51.
8. Patel ZS, Yamamoto M, Ueda H, Tabata Y, Mikos AG. Biodegradable gelatin microparticles as delivery systems for the controlled release of bone morphogenetic protein–2. Acta Biomater. 2008;4(5):1126–38.
9. Lee JY, Kim KH, Shin SY, Rhyu IC, Lee YM, Park YJ, et al. Enhanced bone formation by transforming growth factor-beta1-releasing collagen/chitosan microgranules. J Biomed Mater Res A. 2006;76(3):530–9.
10. Mercier NR, Costantino HR, Tracy MA, Bonassar LJ. Poly(lactide-co-glycolide) microspheres as a moldable scaffold for cartilage tissue engineering. Biomaterials. 2005;26(14):1945–52.
11. Silva GA, Coutinho OP, Ducheyne P, Shapiro IM, Reis RL. The effect of starch and starch-bioactive glass composite microparticles on the adhesion and expression of the osteoblastic phenotype of a bone cell line. Biomaterials. 2007;28:326–34.
12. Link DP, van den Dolder J, van den Beucken JJ, Cuijpers VM, Wolke JG, Mikos AG, et al. Evaluation of the biocompatibility of calcium phosphate cement/PLGA microparticle composites. J Biomed Mater Res A. 2008;87(3):760–9.
13. Conti B, Giunchedi P, Genta I, Conte U. The preparation and in vivo evaluation of the wound healing properties of chitosan microspheres. STP Pharma Sci. 2000;10:101–4.
14. Jayasuriya AC, Bhat A. Optimization of scaled-up chitosan microparticles for bone regeneration, biomedical materials (in review).
15. Rosen CJ, Dimai HP, Vereault D, Donahue LR, Beamer WG, Farley J, et al. Circulating and skeletal insulin-like growth factor-I (IGF-1) concentrations in two inbred strains of mice with different bone mineral densities. Bone. 1997;21:217–23.
16. Hock JM, Centrella M, Canalis E. Insulin-like growth factor I (IGF-1) has independent effects on bone matrix formation and cell replication. Endocrinology. 1988;122:254–60.
17. Jayasuriya AC, Shah C. Controlled release of insulin like growth factor-1 and bone marrow stromal cell function of bone-like mineral layers coated PLGA scaffolds. J Tissue Eng Regen Med. 2008;2(1):43–9.
18. Wang X, Ma J, Wang Y, He B. Structural characterization of phosphorylated chitosan and their applications as effective additives of calcium phosphate cements. Biomaterials. 2001; 22:2247–55.
19. Rehman I, Bonfield W. Characterization of hydroxyapatite and carbonated apatite by photo acoustic FTIR spectroscopy. J Mater Sci: Mater Med. 1997;8(1):1–4.
20. Shin K, Jayasuriya AC, Kohn DH. Effect of ionic activity products on the structure and composition of the mineral formed on 3-D poly(lactic-co-glycolide) scaffolds. J Biomed Mater Res A. 2007;83(4):1076–86.
21. Stigter M, de Groot K, Layrolle P. Incorporation of tobramycin into biomimetic hydroxyapatite coating on titanium. Biomaterials. 2002;23:4143–53.
22. Ohgushi H, Caplan AI. Stem cell technology and bioceramics: from cell to gene engineering. J Biomed Mater Res. 1999;48(6):913–27.
23. Machwate M, Zerath E, Holy X, Pastoureau P, Marie PJ. Insulin-like growth factor-I increases trabecular bone formation and osteoblastic cell proliferation in unloaded rats. Endocrinology. 1994;134(3):1031–8.
24. Boudignon BM, Bikle DD, Kurimoto P, Elalieh H, Nishida S, Wang Y, et al. Insulin-like growth factor I stimulates recovery of bone lost after a period of skeletal unloading. J Appl Physiol. 2007;103(1):125–31.
25. Xu JW, Zaporojan V, Peretti GM, Roses RE, Morse KB, Roy AK, et al. Injectable tissue-engineered cartilage with different chondrocyte sources. Plast Reconstr Surg. 2004;113(5):1361–71.
26. Mercier NR, Costantino HR, Tracy MA, Bonassar LJ. A novel injectable approach for cartilage formation in vivo using PLG microspheres. Ann Biomed Eng. 2004;32(3):418–29.